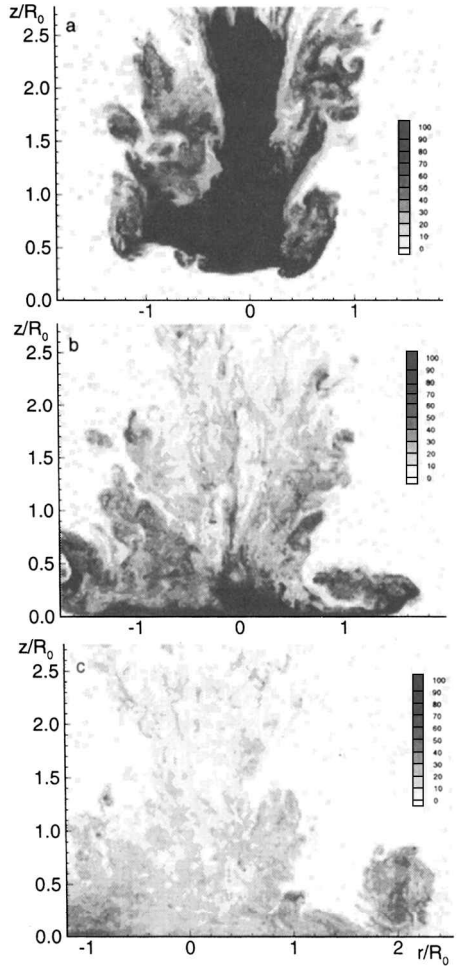

Fig. 2 Concentration fields: a) $4.96T_0$, b) $6.06T_0$, and c) $7.16T_0$ ($H_0 = 3.81R_0$, $Re = 3.6 \times 10^3$; levels represent percentage of heavy fluid).

The experimental concentration fields can be compared with interface contours computed by Lundgren et al.[5] using an inviscid vortex method. In the computations, heavy and light fluid were separated by an interface that stretched and rolled up as the microburst developed. All of the heavy fluid moved quickly to the leading edge of the downdraft, and ambient fluid was entrained from above and wrapped into the core. By the time of ring impact, the largest downdraft velocities were associated with this trailing ambient fluid. No heavy fluid was present in the wake of the ring. The experimental results are similar in that strong downflows persist after passage of the heavy fluid. In contrast, however, the experiment shows significant amounts of heavy fluid remaining in the downdraft column when the vortex ring impacts. Also, significant mixing occurs as a result of shear-driven instabilities at the interface between the light and heavy fluids. Different initial and boundary conditions (shape of initial microburst parcel, release mechanism, and vorticity distribution) in the experimental and numerical flows are probably the most important causes for differences in the results.

Conclusions

In experimental microbursts, heavy fluid wraps into a large vortex near the microburst front. Just before microburst impact, most of the heavy fluid trails the vortex and is associated with large downward velocities. The concentration of heavy fluid remains high in the vortex core and near the ground as the microburst expands radially. Local velocity maxima and gradient maxima are not always associated with heavy fluid, especially when the microburst is most hazardous. Because most ambient fluid is entrained from upstream, velocity maxima and strong horizontal gradients often trail local concentration maxima. Therefore, look-ahead sensing strategies for microburst prediction should not rely exclusively on single-point correlations between velocity and temperature measurements, but multiple-point correlations may be possible.

Acknowledgment

This work was funded by the National Science Foundation (CTS-9209948).

References

[1]Fujita, T. T., "Microbursts as an Aviation Wind Shear Hazard," *Proceedings of the AIAA 19th Aerospace Sciences Meeting* (St. Louis, MO), AIAA, New York, 1981, p. 9 (AIAA Paper 81-0386).

[2]Fujita, T. T., *The Downburst*, Univ. of Chicago Press, Chicago, IL, 1985.

[3]Wilson, J. W., Roberts, R. D., Kessinger, C., and McCarthy, J., "Microburst Wind Structure and Evolution of Doppler Radar for Airport Wind Shear Detection," *Journal of Climate and Applied Meteorology*, Vol. 23, No. 6, 1984, pp. 898–915.

[4]Proctor, F. H., "Numerical Simulation of an Isolated Microburst, Part 1: Dynamics and Structure," *Journal of Atmospheric Sciences*, Vol. 45, No. 21, 1988, pp. 3137–3160.

[5]Lundgren, T. S., Yao, J., and Mansour, N. N., "Microburst Modelling and Scaling," *Journal of Fluid Mechanics*, Vol. 239, 1992, pp. 461–488.

[6]Alahyari, A. A., and Longmire, E. K., "Dynamics of Experimentally Simulated Microbursts," *AIAA Journal*, Vol. 33, No. 11, 1995, pp. 2128–2136.

[7]Lewis, M. S., "Sensing a Change in the Wind," *Aerospace America*, Vol. 31, No. 3, 1993, pp. 20–24.

[8]Alahyari, A., and Longmire, E. K., "Particle Image Velocimetry in a Variable Density Flow: Application to a Dynamically Evolving Microburst," *Experiments in Fluids*, Vol. 17, No. 6, 1994, pp. 434–440.

G. Laufer
Associate Editor

Vortex Breakdown over Unsteady Delta Wings and Its Control

H. Yang* and I. Gursul†
University of Cincinnati, Cincinnati, Ohio 45221-0072

Introduction

THE unsteady aerodynamics of delta wings at high angle of attack has been the subject of several reviews.[1–3] In this Note, control of leading-edge vortices and vortex breakdown over a pitching delta wing with variable sweep are considered. When sweep-angle variations and pitching motion are combined with a proper phase angle, the amplitude of the variations of breakdown location becomes a minimum.

Several experimental studies of vortex breakdown in unsteady flows have shown that the dynamic response of the vortex breakdown location is characterized by time-lag effects. For example, the breakdown location exhibits a phase shift relative to wing motion for a periodically pitching delta wing.[4] The dynamic response of breakdown location is related to the two important parameters that determine the breakdown location: swirl angle and external pressure gradient outside the vortex core. It has been suggested that the dynamic response of vortex breakdown over a pitching delta wing can be explained by the variations of the external pressure gradient.[5] Unsteady pressure measurements indicate that the observed time lag of breakdown location is strongly linked to the external pressure gradient generated by the wing. Hall[6] showed that small external pressure gradients can be amplified along the core of the vortices, leading to a

Received April 29, 1996; revision received Oct. 25, 1996; accepted for publication Nov. 8, 1996; also published in *AIAA Journal on Disc*, Volume 2, Number 2.

*Graduate Student, Department of Mechanical, Industrial, and Nuclear Engineering.

†Assistant Professor, Department of Mechanical, Industrial, and Nuclear Engineering. Member AIAA.

stagnation point. Thus, the large sensitivity of the vortex breakdown location to a streamwise pressure gradient along the exterior of the vortex is very much expected. Nevertheless, the conclusion regarding the role of the external pressure gradient needs to be supported by measurements of flowfield and swirl angle. One objective of this work is to provide information about the variation of swirl angle.

The second objective is the control of leading-edge vortices. For this purpose, leading-edge vortices and vortex breakdown over a delta wing with variable sweep was investigated by flow visualization and laser Doppler velocimetry (LDV) measurements. Periodic variations of the sweep angle are used to control breakdown location for a pitching delta wing.

Experimental Setup

Experiments were carried out in a water channel with a cross-sectional area of 61 × 61 cm. The delta-wing model with variable sweep and the experimental setup are discussed in detail elsewhere.[7,8] The chord length of the wing is $c = 268$ mm, and the Reynolds number based on the chord length is around $Re = 5 \times 10^5$. The range of sweep angle is $\Lambda = 60$ to 70 deg. Two thin plates were used to change the sweep angle. The motion of the plates was guided with a cable that was attached to a drum driven by a dc motor position control system. By using a sine wave input from a function generator, harmonic variations of sweep angle Λ could be obtained for any desired mean, amplitude, and frequency. A variable-speed dc motor and a speed controller were used to drive the pitching mechanism. For the combined motion of pitching and harmonic variations of sweep angle, the input signal to the dc motor position control system was obtained by applying a phase shift to the displacement transducer signal from the pitching mechanism. This provided the desired phase angle between angle of attack $\alpha(t)$ and sweep angle $\Lambda(t)$.

Flow visualization of vortex breakdown was done by injecting fluid with food-coloring dye near the apex of the model. The velocity was measured with a single-component LDV system operating in the backscattering mode. The measurement volume size is about 0.08 mm in diameter and 0.65 mm long. The measurement uncertainty for the mean velocity was estimated as 1%. Phase-averaging technique was applied to the velocity signals for the periodic variations of sweep angle and angle of attack. Because the LDV system has the capability of measuring a single component of velocity, the swirl-velocity component was measured separately by rotating the optical probe and applying the phase-averaging technique, which is discussed in detail elsewhere.[9]

Results

The variation of breakdown location was studied for harmonic variations of sweep angle, $\Lambda = \Lambda_0 + \Lambda_1 \sin \omega t$. Experiments were conducted for different values of mean sweep angle Λ_0 and amplitude Λ_1 at fixed angles of attack and summarized by Yang.[9] The variations of the ensemble-averaged breakdown location as a function of sweep angle showed hysteresis loops, which was an indication of the existence of phase lags. An example is shown in Fig. 1a for $\Lambda_0 = 66$ deg and $\Lambda_1 = 3$ deg at $\alpha = 20$ deg. The reduced frequency is $k = \omega c / 2U_\infty = 0.4$, where ω is the radial frequency and U_∞ is the freestream velocity. Note that a relatively large phase lag (about 85 deg) of breakdown location exists with respect to the sweep-angle variations. Although the phase delay of breakdown location increases with increasing reduced frequency for pitching delta wings, the phase delay is not a monotonic function of reduced frequency for sweep-angle variations.[8]

To understand the phase lag of vortex breakdown, phase-averaged velocity measurements were carried out in a cross plane (at $x/c = 0.5$) upstream of breakdown location to obtain the variations of the upstream conditions. The variation of the swirl angle $\phi = \tan^{-1}(v/u)$, where v is the swirl velocity and u is the axial velocity, with the distance from the vortex axis is qualitatively similar to that of swirl velocity: zero at the vortex axis and a local maximum at the edge of the subcore.[9] The maximum value of the swirl angle is traditionally used to characterize the magnitude of swirl. Variation of maximum swirl angle over one cycle is shown in Fig. 1b. It is clear that the phase lag of the maximum swirl angle with respect to the quasisteady case is very small. Therefore, it confirms that when the sweep angle is varied dynamically, the unsteady effects upstream

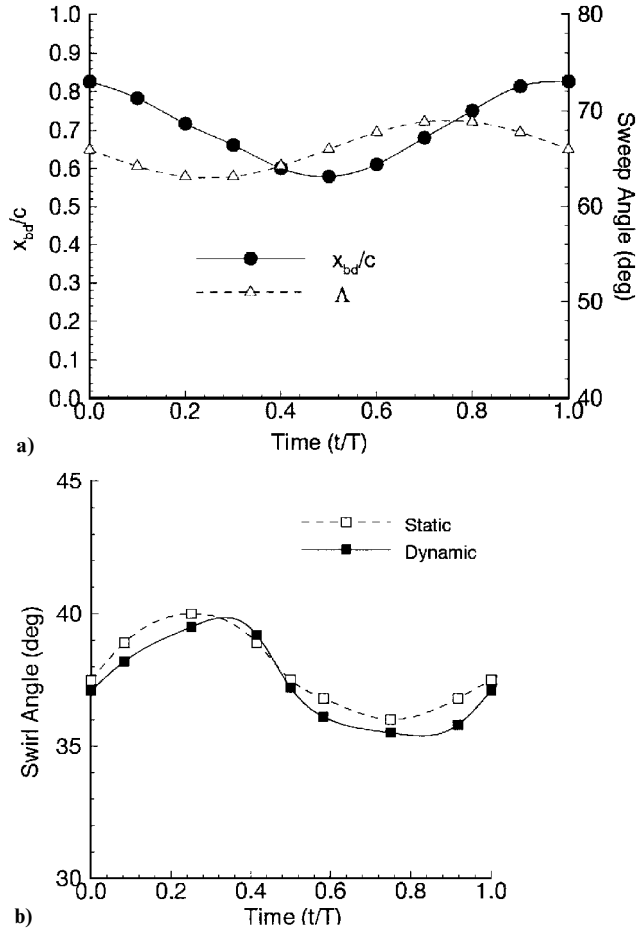

Fig. 1 Variation of a) breakdown location and b) maximum swirl angle over one cycle for harmonic variations of sweep angle: $\Lambda_0 = 66$ deg, $\Lambda_1 = 3$ deg, $\alpha = 20$ deg, and $k = 0.4$.

of breakdown location are not very strong. This suggests that the variations of the external pressure gradient (which is the other of the two control parameters for breakdown) should be responsible for the large phase lag of vortex breakdown location.

Perturbations applied at the leading edge by varying sweep angle dynamically around a mean value may provide an effective way for breakdown control in unsteady flows. To demonstrate this, the pitching motion of the delta wing for a fixed sweep angle was considered: $\alpha = \alpha_0 + \alpha_1 \sin \omega t$. First, the pitching motion was studied as a reference case. Variation of ensemble-averaged breakdown location with time for $\alpha_0 = 20$ deg and $\alpha_1 = 5$ deg (for a fixed value of sweep angle $\Lambda = 66$ deg and $k = 0.4$) over one cycle and for the static case is presented in Fig. 2a. The phase lag of the variation of breakdown location is approximately 40 deg.

Phase-averaged velocity measurements also were carried out in a cross plane at $x/c = 0.5$ upstream of breakdown location. The variation of maximum swirl angle was obtained from the phase-averaged axial and swirl velocity measurements (Fig. 2b). There is a very small phase lag (about 10 deg) in the variation of maximum swirl angle. This phase lag is much smaller than the phase lag of breakdown location. Similar to the case of sweep-angle variations, it is concluded that the variations of the external pressure gradient should be responsible for the large phase lag of vortex breakdown location. In fact, it was shown in an earlier work that the phase delay of the variation of the external pressure gradient is very close to that of the variation of breakdown location.[5] In summary, the swirl angle makes a small contribution to the phase delay of vortex breakdown location, but the variations of external pressure gradient play a major role. The fact that the external pressure gradient generated by the wing itself plays a major role in the dynamic response of breakdown location also was suggested for a delta wing in an unsteady freestream.[10]

The perturbations of the sweep angle with the same frequency as pitching, but with a phase angle present, are considered: $\alpha =$

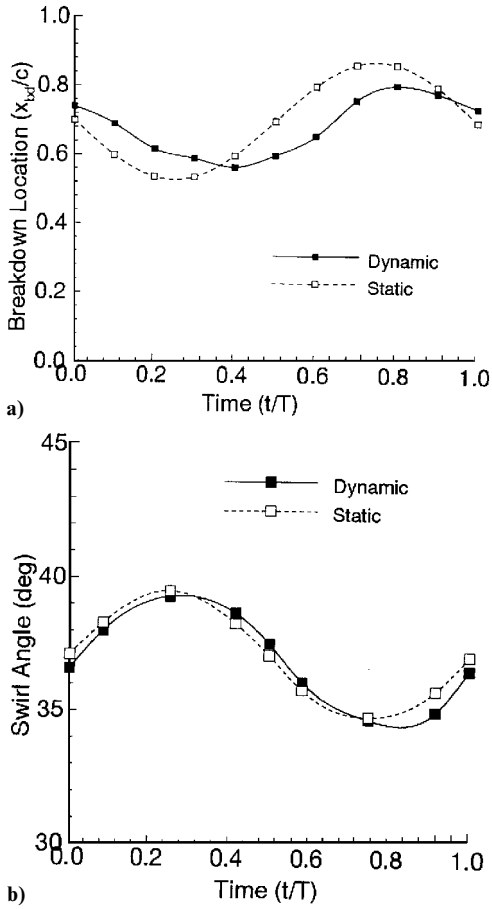

Fig. 2 Variation of a) breakdown location and b) maximum swirl angle for pitching motion: $\alpha_0 = 20$ deg, $\alpha_1 = 5$ deg, $\Lambda = 66$ deg, and $k = 0.4$.

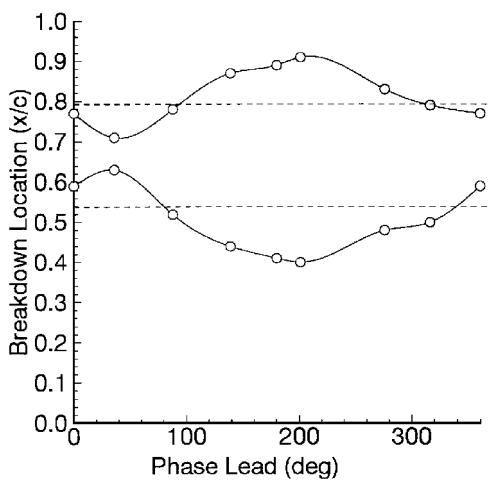

Fig. 3 Maximum and minimum breakdown locations as a function of phase angle; the dashed lines are for pitching motion only for the average sweep angle: $\alpha_0 = 20$ deg, $\alpha_1 = 5$ deg, $\Lambda_0 = 66$ deg, $\Lambda_1 = 3$ deg, and $k = 0.4$.

$\alpha_0 + \alpha_1 \sin \omega t$ and $\Lambda = \Lambda_0 + \Lambda_1 \sin(\omega t + \Phi)$. The variation of the ensemble-averaged breakdown location strongly depends on the phase angle Φ, which was varied over a range of 360 deg, and the maximum and minimum values of breakdown location during a cycle were documented. Several cases were tested by varying α_0, α_1, Λ_0, Λ_1, and k, as tabulated by Yang.[9] The variation of maximum and minimum breakdown locations as a function of phase angle is shown in Fig. 3 for $\Lambda_0 = 66$ deg, $\Lambda_1 = 3$ deg, $\alpha_0 = 20$ deg, and $\alpha_1 = 5$ deg. The amplitude of the variations decreases considerably at an optimum phase angle around 35 deg. The dashed lines indicate the maximum and minimum locations for the pitching motion only at the average sweep angle Λ_0.

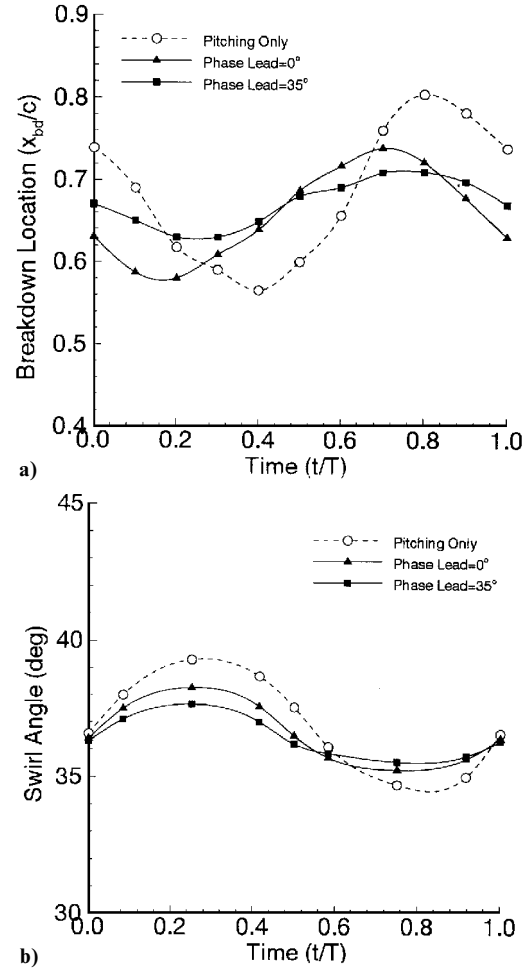

Fig. 4 Variation of a) breakdown location and b) maximum swirl angle for combined motion: $\alpha_0 = 20$ deg, $\alpha_1 = 5$ deg, $\Lambda_0 = 66$ deg, $\Lambda_1 = 3$ deg, and $k = 0.4$.

For the case shown in Fig. 3, detailed phase-averaged measurements were carried out. Two different values of phase lead were considered: $\Phi = 0$ and 35 deg (the optimal phase lead). The results were compared with that of pitching motion only (at average sweep angle $\Lambda_0 = 66$ deg). First, variations of phase-averaged breakdown location are compared in Fig. 4a. It is clear that the amplitude of variation of breakdown location is minimum for the optimal phase lead. Another important feature is that the large phase lag of breakdown location in the pitching motion vanishes in the combined motion for $\Phi = 35$ deg. Recall that the phase delay of breakdown location is strongly related to the external pressure gradient. Therefore, it is concluded that harmonic variations of sweep angle with proper phase lead modify the variation of the external pressure gradient. Phase-averaged axial and swirl velocities were measured to document upstream conditions (at $x/c = 0.5$). The variation of the maximum swirl angle is shown in Fig. 4b. The decrease in the amplitude of maximum swirl angle due to the perturbations of sweep angle is evident. Again, for the optimal phase lead, the amplitude is smallest, which is consistent with the smallest amplitude of breakdown location.

Conclusions

The variation of vortex breakdown location for harmonic variations of sweep angle showed hysteresis loops and phase lags that depend on the reduced frequency. However, the variation of swirl angle revealed very small phase lag compared to the large phase lag of breakdown location, suggesting that the external pressure gradient plays a major role in the dynamic response of breakdown location. Similar results were obtained for a pitching delta wing. The swirl angle has a small phase delay, but the variations of the external pressure gradient play a major role, as shown earlier by the pressure measurements.

Use of variable sweep for breakdown control was demonstrated for a pitching delta wing. Oscillations of sweep angle with the same frequency as pitching were considered, but with a phase angle. It was shown that, at an optimum phase angle, the amplitude of the variations of breakdown location becomes a minimum. For the optimum phase angle, the amplitude of the swirl angle decreases considerably.

Acknowledgment

This research was supported by U.S. Air Force Office of Scientific Research Grant F49620-92-J-0532.

References

[1]Lee, M., and Ho, C.- M., "Lift Force of Delta Wings," *Applied Mechanics Reviews*, Vol. 43, No. 9, 1990, pp. 209–221.

[2]Rockwell, D., "Three-Dimensional Flow Structure on Delta Wings at High Angle-of-Attack: Experimental Concepts and Issues," AIAA Paper 93-0550, Jan. 1993.

[3]Visbal, M. R., "Computational and Physical Aspects of Vortex Breakdown on Delta Wings," AIAA Paper 95-0585, Jan. 1995.

[4]LeMay, S. P., Batill, S. M., and Nelson, R. C., "Vortex Dynamics on a Pitching Delta Wing," *Journal of Aircraft*, Vol. 27, No. 2, 1990, pp. 131–138.

[5]Gursul, I., and Yang, H., "Vortex Breakdown over a Pitching Delta Wing," *Journal of Fluids and Structures*, Vol. 9, 1995, pp. 571–583.

[6]Hall, M. G., "Vortex Breakdown," *Annual Review of Fluid Mechanics*, Vol. 4, 1972, pp. 195–218.

[7]Gursul, I., Srinivas, S., and Batta, G., "Active Control of Vortex Breakdown over a Delta Wing," *AIAA Journal*, Vol. 33, No. 9, 1995, pp. 1743–1745.

[8]Gursul, I., Yang, H., and Deng, Q., "Control of Vortex Breakdown with Leading-Edge Devices," AIAA Paper 95-0676, Jan. 1995.

[9]Yang, H., "Unsteady Nature of Vortex Breakdown over Delta Wings and Its Control," Ph.D. Thesis, Dept. of Mechanical, Industrial, and Nuclear Engineering, Univ. of Cincinnati, OH, 1996.

[10]Gursul, I., and Ho, C.-M., "Vortex Breakdown over Delta Wings in Unsteady Freestream," *AIAA Journal*, Vol. 32, No. 2, 1994, pp. 433–436.

A. Plotkin
Associate Editor

Approximating Collisional Freestream Attenuation at Transitional Knudsen Numbers

Lyon B. King* and Alec D. Gallimore†
University of Michigan, Ann Arbor, Michigan 48109

Nomenclature

C_1 = arbitrary constant
F = velocity distribution function
f = normalized velocity distribution function
I = total number of scattered molecules
k = Boltzmann constant 1.38×10^{-23} J/kg K
L = collision interaction length, m
m = mass of molecule, kg
n_m = measured number density, m^{-3}
n_1 = number density of class 1 molecules, m^{-3}
n_2 = number density of class 2 molecules, m^{-3}
n_{1o} = number density of class 1 molecules at plate surface, m^{-3}
n_{2o} = number density of class 2 molecules in freestream, m^{-3}
q = dynamic pressure, Pa
T_p = plate surface temperature, K
u_o = bulk velocity of freestream, m/s
v_n = velocity normal to plate surface, m/s
x = streamwise position coordinate, m
δ = Dirac function
κ = pressure amplitude constant [Eq. (13)]
λ = mean free path, m
σ_{12} = total collision cross section, m^2
$\Phi_i^{(x)}$ = incident flux of quantity x
$\Phi_r^{(x)}$ = reflected flux of quantity x

Received April 2, 1996; revision received Oct. 17, 1996; accepted for publication Nov. 6, 1996; also published in *AIAA Journal on Disc*, Volume 2, Number 2.

*Graduate Student Researcher, Plasmadynamics and Electric Propulsion Laboratory, Department of Aerospace Engineering. Student Member AIAA.

†Assistant Professor, Plasmadynamics and Electric Propulsion Laboratory, Department of Aerospace Engineering. Member AIAA.

Introduction

When a body such as an instrument package is immersed within a rarefied flowfield, the inevitable result is distortion of the freestream. This perturbation is a formidable stumbling block for code developers seeking reliable experimental data for comparison with flowfield predictors. A special interest of late has been the determination of the true freestream dynamic pressure for an exoatmospheric plume. This effort has been inspired by the desire to create an accurate plume flowfield predictor for the Space Shuttle Orbiter's primary reaction control thrusters.[1] Current codes produce a spatial map of dynamic pressure. Validation of the codes must rely on an accurate means of determining the undisturbed freestream dynamic pressure from experimental data for comparison. Although this problem is closed for a continuum case via the Rayleigh–Pitot formula, the extreme low density inherent to an exoatmospheric plume renders this treatment invalid because the thickness of the shock layer may be many times larger than the body immersed in the flow.

Analytical Model

The basic approach taken to solve this problem was to analyze the interaction between two separate streams of molecules. Molecule class 2 represents the undisturbed freestream of the thruster plume; molecule class 1 represents the molecules that previously have impacted the plate and have been reflected from its surface. The positive x direction is taken toward the plate, parallel with the freestream velocity. The location of $x = 0$ corresponds with the outermost edge of the defined collision zone, with $x = L$ coincident with the plate surface. The assumptions utilized in the model are presented here a priori and will be referenced throughout the solution.

1) *The directed bulk flow velocity is high in comparison with the random thermal velocity within the freestream molecules (very large speed ratio).* A Dirac probability density function will preselect molecules with this limiting velocity while not allowing molecules with any other speeds: $F_2 = n_2\delta(v_z)\delta(v_y)\delta(v_x + u_0)$.

2) *Molecules impacting the plate are fully accommodated and reemitted in thermal equilibrium with the plate (diffuse reflection).* The result of this assumption is that molecules reflected from the plate will have a half-Maxwellian distribution, F_1, at temperature T_p and density n_{1o}.

3) *The velocity of class 2 molecules is much greater than that of class 1 molecules.* This assumption requires the velocity of the freestream molecules to be much greater than the thermal speed of the Maxwellian plate molecules. Utilizing assumption 1, this requires $u_0 \gg (kT_p/\pi m)^{1/2}$.

The remaining assumptions (presented below) pertain to the intermolecular collision phenomena of the transitional flow regime. In this regime the theory takes on the form of a First-Collision Theory, accounting for some molecular collisions while neglecting other collisions. In this First-Collision treatment of the problem, the following assumptions were made:

4) *Intermolecular collisions are characterized by hard-sphere interactions.*

5) *Class 1 molecules are collisionless with respect to other class 1 molecules. Similarly, class 2 molecules are collisionless with respect to other class 2 molecules. The only collisions of significance are those arising between class 1 and class 2 molecules.*

6) *Any collision between a class 1 and a class 2 molecule causes both molecules to be scattered such that neither molecule intersects with the plate surface. In addition, these scattered molecules do not*